

# Removal of Remazol Yellow

*by Fahma Riyanti*

---

**Submission date:** 27-Apr-2023 07:38PM (UTC+0700)

**Submission ID:** 2077115686

**File name:** Removal\_of\_Remazol\_10\_JST-april22.pdf (1.48M)

**Word count:** 5688

**Character count:** 30308

## Removal of Remazol Yellow Using SnO<sub>2</sub>-Co Photocatalyst

Muhammad Said<sup>1,2\*</sup>, Fahma Riyanti<sup>1,2</sup>, Poedji Loekitowati Hariani<sup>1,2</sup>, Sastriani<sup>1</sup> and Widya Twiny Rizki<sup>3</sup>

<sup>1</sup>Department of Chemistry, Faculty of Mathematics and Natural Science, Sriwijaya University, 30662, South Sumatra, Indonesia

<sup>2</sup>Research Centre of Advanced and Nanocomposite, Sriwijaya University, 30662, South Sumatra, Indonesia

<sup>3</sup>Magister Program of Chemistry, Faculty of Mathematics and Natural Science, Sriwijaya University, 30662, South Sumatra, Indonesia

### ABSTRACT

Remazol yellow is a synthetic dye that pollutes the environment and causes disease because it is carcinogenic and mutagenic. Photocatalyst is one of the technologies to remove the dye concentration, and tin oxide (SnO<sub>2</sub>) with cobalt (Co) dopant has the potential to be a good semiconductor in the process. Therefore, this study aims to synthesize SnO<sub>2</sub>/Co composites as a photocatalyst to degrade Remazol yellow dye. The photodegradation process was carried out with several variables, including the effect of time and the initial concentration of the dye and conditions under pH<sub>pzc</sub>. Furthermore, the composites were made with SnO<sub>2</sub> to Co mass ratios of (2:1), (2:2), (2:3), and were characterized using X-Ray Diffraction (XRD), Scanning Electron Microscope-Energy Dispersive X-Ray (SEM-EDX), and Ultraviolet-Visible Diffuse Reflectance Spectroscopy (UV-Vis DRS) instruments. Based on the results, the SnO<sub>2</sub>/Co (2:3) composite was selected as a photocatalyst to degrade the dye as the XRD characterization showed the formation of a typical peak of 2θ at 33°. The energy bandgap of SnO<sub>2</sub> is 3.05 eV, while the (2:3) composite had a value of 2.8eV. Moreover, the SEM characterization showed a non-uniform surface with pores

and elements composition of Sn, O, and Co with the values 61.24, 24.67, and 14.09 wt%, respectively. The optimum condition for photodegradation was obtained at a contact time and concentration of 180 minutes and 10 ppm, respectively, while the removal of the dye reached 65-80%.

**Keywords:** Concentration, contact time, photocatalyst, Remazol yellow, SnO<sub>2</sub>/Co

### ARTICLE INFO

#### Article history:

Received: 12 November 2021

Accepted: 14 February 2022

Published: 20 April 2022

DOI: <https://doi.org/10.47836/pjst.30.3.10>

#### E-mail addresses:

msaidusman@unsri.ac.id (Muhammad Said)

sastriani542@gmail.com (Sastriani)

widyatwinirizki@gmail.com (Widya Twiny Rizki)

fatechafj@yahoo.com (Fahma Riyanti)

puji\_loekitowati@mipa.unsri.ac.id (Poedji Loekitowati Hariani)

\* Corresponding author

ISSN: 0128-7680

e-ISSN: 2231-8526

© Universiti Putra Malaysia Press

## INTRODUCTION

Azo compounds and their derivatives in the form of benzene groups are one of the main sources of environmental pollution caused by dyes. One of these compounds is Remazol yellow FG, a synthetic dye often used in the batik industry (Handayani et al., 2016). However, it pollutes the environment and potentially causes disease due to its carcinogenic and mutagenic properties. Several studies have been carried out on the processing of color wastes using the adsorption method (Guezzen et al., 2018), with the bacteria *Pseudomonas sp* (Shah et al., 2013) and the photocatalyst method (Ba-Abbad et al., 2017). Photocatalyst utilizes semiconductor materials and light energy, from sunlight and UV lamps, to degrade dye waste. Light energy is used to activate a catalytic process on the surface of semiconductor materials to produce free electrons and holes (Bouaine et al., 2007). The electron-holes formed will migrate to the semiconductor surface and then react with  $O_2$  and  $H_2O$  to form reactive oxidation species ( $O_2^-$  and  $\cdot OH$ ), capable of oxidizing the organic molecules (Mohammed et al., 2017). The photocatalytic degradation process can be operated under room temperature and atmospheric pressure and mineralize organic molecules into environment-friendly products (Akti, 2018).

Different studies on semiconductor materials as photocatalysts have been reported, including Sudha and Sivakumar (2015), which used ZnO,  $TiO_2$ ,  $WO_3$ , and  $SnO_2$  as semiconductors. Tin oxide ( $SnO_2$ ) is a semiconductor oxide material with good potential as a photocatalyst as it has good optical properties and electrical conductivity, wide surface area, high physicochemical stability, small energy bandgap, environmentally friendly, and non-destructive (Mani et al., 2016). Meanwhile,  $SnO_2$  photocatalytic ability to degrade dye is increased by modification, such as the addition of metal dopants (Malvankar et al., 2020). Generally, the metal commonly used as a dopant is cobalt (Co) with various concentrations, as Pirmoradi et al. (2011) reported, which used the sol-gel method in the doping process. The result showed a decrease in the energy bandgap from 3.19 eV to 2.97 eV. The addition of dopant Co to  $SnO_2$  was also carried out by Wan et al. (2016), and a homogeneous distribution of the metal particles on the semiconductor surface was found. Moreover, this process affects the crystal size of  $SnO_2$ -Co. The smaller the crystal size, the larger the surface area, thereby increasing the degradation and adsorption performance of the crystals (Attar, 2018).  $SnO_2$ -Co composites are widely used for various purposes such as gas sensor applications (Rukkumani et al., 2017), antibacterial studies (Qamar et al., 2017), and dye degradation (Naje et al., 2013).

The photocatalytic degradation of synthetic dyes was carried out by Sivakarathik et al. (2016), which used  $SnO_2$ -Co to degrade methyl violet and obtained 60–70% degradation with the optimum time of 200–225 minutes using sunlight irradiation. The photocatalytic degradation using  $SnO_2$ -Co was also used by Ragupathy and Ramamoorthy (2021) to degrade methylene blue dye and obtained an efficiency degradation of 95.38%. Furthermore, Remazol yellow photocatalytic degradation studies using various photocatalysis have been

reported. Pumawan et al. (2021) used TiO<sub>2</sub> doped Cd, Co, and Mn. The highest percentages degradation for 30 minutes (74.61%) was achieved using TiO<sub>2</sub>-Co. Bhuiyan et al. (2020) used iron oxide extracted from *Carica papaya* leaf. The optimum conditions were obtained at a catalyst dose of 0.8 g/L, pH of 2, for 6 hours with a maximum color degradation of 76.6%. Akti (2018) used Polyaniline doped SnO<sub>2</sub>-diatomite. It was found that the use of a catalyst dose of 1 g/L in 1 hour resulted in a degradation achieved of 96%. Akti and Balci (2022) used APTES (3-aminopropyl triethoxysilane) and ethyl alcohol modified Sn/SBA-15. The study showed that the Remazol yellow degradation was obtained up to 58.2%. According to the literature review, studies on photocatalytic degradation of Remazol red using SnO<sub>2</sub>-Co semiconductor have not been well reported. Therefore, this study aims to synthesize and modify the semiconductor of SnO<sub>2</sub> doped with cobalt (SnO<sub>2</sub>-Co) for Remazol red photodegradation. It was conducted with several variables, including the effect of degradation time and the initial concentration of the dye, while the characterizations used to test the material were XRD (X-ray diffraction), SEM (scanning electron microscopy), and UV-Vis DRS (UV-vis diffuse reflectance spectroscopy).

## METHODS

### SnO<sub>2</sub> Preparation

3 g of SnCl<sub>2</sub> was dissolved in 150 mL of distilled water and stirred for 1 hour, then NH<sub>4</sub>OH solution was added dropwise with constant stirring until it reached pH 7. The gel produced was filtered and dried in an oven at 80°C for 24 hours to remove water molecules (Naje et al., 2013). The powder obtained was characterized using XRD, SEM, and DRS instruments.

### Synthesis of SnO<sub>2</sub>-Co with Variation in the Concentration of Doping Materials

2 g of SnO<sub>2</sub> powder was added with Co(NO<sub>3</sub>)<sub>2</sub> with various concentration ratios of 2:1; 2:2, 2:3, and then dissolved in 100 mL of distilled water with constant stirring for 1 hour. Furthermore, NaOH solution was added dropwise with constant stirring until a pH of 7 was reached. The solution was filtered, while the filtrate was mixed with ethanol, precipitated, and then filtered. The precipitate was washed and dried in an oven at 400°C for 1 hour, while the powder obtained was used for characterization and photocatalytic examination (Saravanakumar et al., 2016). The characterization was carried out using XRD, DRS, and SEM instruments. The material from the best characterization results was used to degrade the dye.

### Degradation of Remazol Yellow

**Effect of Degradation Time.** The effect of time on the degradation process was determined using a sample solution of 25 ppm Remazol yellow FG. 0.50 g of SnO<sub>2</sub>-Co was added into 1000 mL of beaker glass and 10 mL of Remazol yellow sample solution. The mixture was

stirred with a magnetic stirrer and exposed to a UV lamp (20 watts) with an irradiation time of 30, 60, 90, 120, 150, and 180 minutes in the radiation box. Furthermore, the degraded dye solution was centrifuged for 20 minutes at a speed of 3000 rpm to separate SnO<sub>2</sub>-Co from the solution. 1 mL of the solution was then taken, and the absorbance was measured using a UV-Vis spectrophotometer at the maximum wavelength with distilled water. The concentration calculation was carried out by entering the absorbance obtained into the standard curve equation for Remazol yellow. As a control, Remazol yellow degradation process was also carried out without UV lamp irradiation with the same variation of contact time.

**Effect of Initial Concentration of Remazol Yellow.** The effect of Remazol yellow dye initial concentration was determined using a standard solution of 10 mL of 10, 15, 20, 25, 30 ppm, respectively. Five beakers of 100 mL were added with 0.50 g of SnO<sub>2</sub>-Co and a standard solution of Remazol yellow FG. The mixture was stirred with a magnetic stirrer and then exposed to a UV lamp (20 watts) in a radiation box to determine the optimum exposure time. The degraded dye solution was centrifuged for 20 minutes at a speed of 3000 rpm to separate SnO<sub>2</sub>-Co from the solution. Furthermore, 1 mL of the solution was taken, and the absorbance was measured using a UV-Vis spectrophotometer at the maximum wavelength with distilled water. The initial concentration was calculated by entering the absorbance obtained into the standard curve equation for the Remazol yellow. As a control, Remazol yellow degradation process was also carried out without UV lamp irradiation with the same variation of initial concentration.

**Data Analysis.** The percent decrease in Remazol yellow FG concentration was calculated using Equation 1 with the triple measurement as follows:

$$P = \frac{C_o - C_t}{C_o} \times 100\% \quad (1)$$

Where,

P = Percentage decrease in solution concentration.

Co = Initial concentration of solution before degradation (ppm).

Ct = concentration of solution after degradation at time t (ppm).

## RESULTS AND DISCUSSIONS

### Characterization of X-Ray Diffraction (XRD)

Characterization using XRD was carried out to identify the crystal's phase, structure, and size type. The results were identified by comparing the formed peaks with data from the

JCPDS card No. 41-1445. SnO<sub>2</sub> and the SnO<sub>2</sub>-Co composite XRD characterization results are shown in Figure 1.

Figure 1(a) shows the results of the SnO<sub>2</sub> material diffractogram, and the 2 $\theta$  angle characterization was compared with the JCPDS card data No.41- 1445. Based on the data, the angle characteristic of 2 $\theta$  SnO<sub>2</sub> is 26.6°; 33.8°; 37.9°; 51.8° 57.9° and 62.0° with field indexes (110), (101), (200), (211), (002) and (310) (Bhagwat et al., 2015). The SnO<sub>2</sub> result showed similarities with JCPDS card No.41-1445 data with a slight shift of the peaks, in angles 26.52°, 32.1°, and 51.8°. Meanwhile, Figure 1(b) shows the result of the SnO<sub>2</sub>-Co (2:1) composite diffractogram with peaks at 2 $\theta$  angles of 33.510°; 37.22°; 57.50°, and 62.38° while the (2:2) composite diffractogram showed peaks at an angle of 2 $\theta$  26.9°; 33,516°; 37.32°; 57.61° and 62.41° as shown in Figure 1(c). Furthermore, the SnO<sub>2</sub> -Co (2:3) sample diffractogram, as presented in Figure 1(d), indicated peaks at angles of 2 $\theta$  26.60°; 33.40°; 37.26°; 51.0°; 57.61° and 62.54°.

The XRD diffractogram results in Figure 1 showed the type of phase produced by the nanocrystalline. The crystal size was below 100 nm with a tetragonal crystal structure as indicated by the formed peaks at a typical angle of 26°, 33°, and 51° (Saravanakumar et al, 2016). Based on Figure 1, in each SnO<sub>2</sub>-Co composite, the highest peak intensity was at 30° 2 $\theta$  angle. According to Lokhand (2015), the diffraction pattern of cobalt doping peaks generally appears at a 2 $\theta$  angle between 20 to 50° with a characteristic diffraction peak at 30°. The highest intensity of the peak at 30° is due to an incomplete reaction which causes excessive reactants and by-products in each of the composite synthesis processes. Another problem Ibarguen et al. (2007) reported was that the formation of a peak at a 30° in the diffraction pattern is caused by the excess amount of NH<sub>4</sub>OH, which makes the pH of

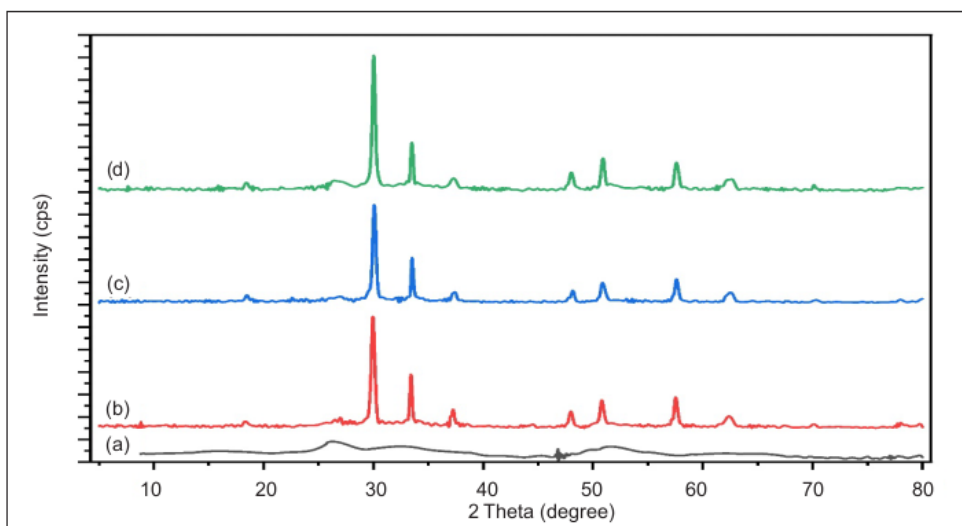


Figure 1. XRD Spectra of (a) SnO<sub>2</sub> (b) SnO<sub>2</sub>-Co (2:1) (c) SnO<sub>2</sub>-Co(2:2) (d) SnO<sub>2</sub>-Co (2:3)

the solution to be alkaline. Therefore, the best XRD characterization from each SnO<sub>2</sub>-Co composite was selected for the photodegradation process. One of the factors to determine the best composite for photodegradation applications is the crystal size. Sharma et al. (2014) reported that crystal size affects photodegradation. As the crystal size increases, the degradation efficiency decreases due to the reduction of the surface area and active sites on the surface of the photocatalyst, which in turn decreases the number of hydroxyl radicals and superoxide. A similar finding has also been reported by Peng et al. (2005) that the small crystal size of the photocatalyst indicated high photocatalytic activity. The SnO<sub>2</sub>-Co crystal size was calculated using the Debye-Scherrer formula, and the (2:1) (2:2) and (2:3) composites have a value of 48.87 nm, 48.80 nm, and 39.61 nm, respectively. Based on the diffractogram and crystal size data, the SnO<sub>2</sub>-Co (2:3) composite was selected for the photodegradation of Remazol yellow because its peaks have a typical angle of 26, 33, and 51°, which are similar to the JCPDS card No.41-1445 data and has the smallest crystal size.

#### **Characterization of UV-Visible Diffuse Reflectance Spectrophotometer (UV-Vis DRS)**

The DRS UV-Vis characterization was carried out to determine the energy bandgap value of SnO<sub>2</sub> and the SnO<sub>2</sub>-Co composite (2:3). In general, semiconductor materials have two energy bands: valence, and conduction. The distance between the valence to the conduction band is called the energy bandgap. The standard value of the energy bandgap of SnO<sub>2</sub> is 3.6 eV (Pirmoradi et al., 2011). The measurement in the SnO<sub>2</sub> and SnO<sub>2</sub>-Co (2: 3) composite with UV-Vis DRS characterization was carried out by providing energy at a wavelength of 200–800 nm. When the electrons in the valence band absorb the appropriate photon energy, then the conduction band is excited. The electrons also transmit some energy back to the ground state, while the transmitted energy by the material is equal to the width of the energy bandgap.

The UV-Vis DRS measurement results of the energy bandgap value of the SnO<sub>2</sub> and SnO<sub>2</sub>-Co composite (2:3) are shown in Figure 2. The energy bandgap of SnO<sub>2</sub> was 3.05 eV, while for SnO<sub>2</sub>-Co was 2.8 eV. The energy bandgap of SnO<sub>2</sub>-Co composite was smaller than SnO<sub>2</sub> due to the influence of doping with Co. This phenomenon was also reported by Mani et al. (2016), which stated that Co metal has a smaller value than Sn; therefore, Co acts as an electron acceptor and decreases the energy bandgap value. The addition of dopant Co to SnO<sub>2</sub> reduced the energy required for electrons to excite from the valence to the conduction band, reducing the bandgap value. Furthermore, Pirmoradi et al. (2011) stated that the addition of cobalt as doping to semiconductors reduces the bandgap energy. Therefore, its application as a photocatalyst was carried out in visible light to reduce energy efficiency. It is caused by cobalt, which acts as an absorber to collect the photoelectrons produced from the semiconductor conduction band.

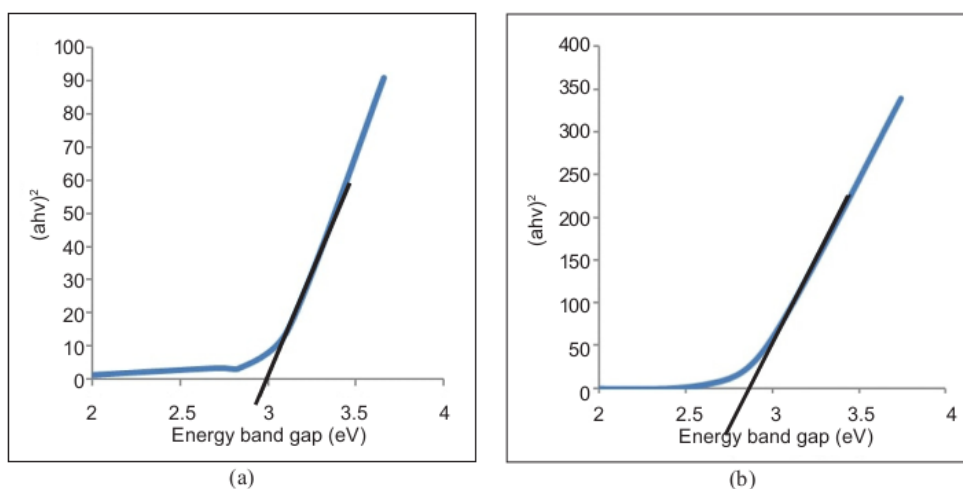


Figure 2. UV-Vis DRS of (a) SnO<sub>2</sub> (b) SnO<sub>2</sub>-Co (2:3)

### Characterization of Scanning Electron Microscopy (SEM)

SEM characterization was carried out to determine the morphological shape of the SnO<sub>2</sub> semiconductor and SnO<sub>2</sub>-Co (2:3) composite to determine the constituent elements. It was performed at 3000x magnification, as shown in Figure 3. The surface morphology presented in Figure 3 (a) showed that the SnO<sub>2</sub> obtained was in the amorphous/crystalline phase. Meanwhile, Yehia et al. (2019) reported that amorphous/crystalline SnO<sub>2</sub> has a distinct porous surface with uneven particles. Furthermore, the surface morphology of the SnO<sub>2</sub>-Co composite demonstrated in Figure 3 (b) showed that the particle size of SnO<sub>2</sub>-Co was bigger than SnO<sub>2</sub>. The SnO<sub>2</sub>-Co composite has a round morphology with an uneven surface. It is due to Co doping which aggregates on the surface of SnO<sub>2</sub> and forms pores, as previously

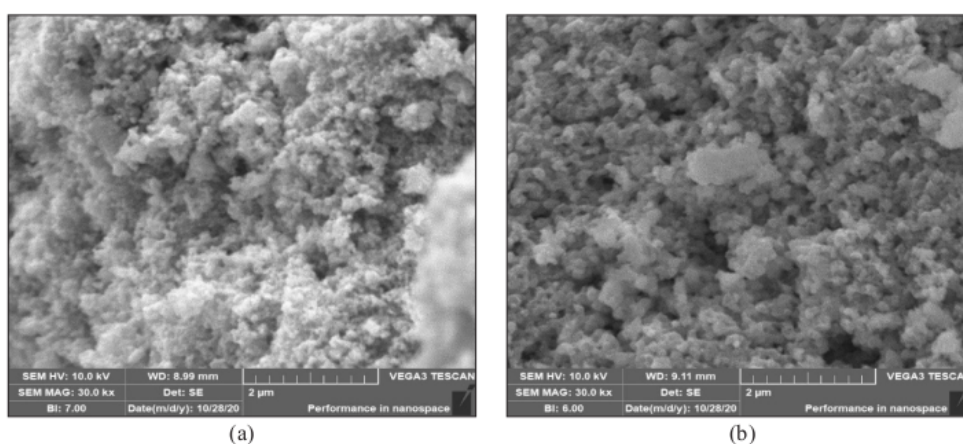


Figure 3. SEM morphology at  $\times 3000$  magnification of (a) SnO<sub>2</sub> surface (b) SnO<sub>2</sub>-Co (2:3)



reported by Sivakhartik et al. (2016). The analysis results of the constituent elements of SnO<sub>2</sub> and SnO<sub>2</sub>-Co composites (2:3) are shown in Table 1.

Based on Table 1, the success of the SnO<sub>2</sub>-Co composite (2:3) was indicated by the presence of Sn, O, and Co elements. The Sn composition, namely 61.24 wt%, was higher than the Co, which was only 14.09 wt% and the presence of O at 24.67

wt% indicates that the composite was successfully synthesized. Meanwhile, the Sn and O percentages in the SnO<sub>2</sub> semiconductor were 62.62 wt% and 29.78 wt%, respectively, which indicates successful synthesis with only a few impurities such as carbon (5.61 wt%) and nitrogen (1.98 wt%).

Table 1  
Composition of the constituent SnO<sub>2</sub> and composite elements SnO<sub>2</sub>/Co (2:3)

	SnO <sub>2</sub> (wt%)	Composite SnO <sub>2</sub> /Co (2:3) (wt%)
Sn	62.63	61.24
O	29.78	24.67
Co	-	14.09
C	5.61	-
N	1.98	-

### pH Point Zero Charge (pHpzc) SnO<sub>2</sub>-Co (2:3) Composite

The pH point zero charges (pH pzc) is the meeting point between the straight lines from the initial to the final pH curve of the solution in a neutral charge state. It is also the point between the initial and final pH after immersion for 24 hours. The pHpzc data is used to determine the appropriate pH conditions for the photodegradation process, as shown in Figure 4.

Figure 4 shows that the pHpzc for the SnO<sub>2</sub>/Co (2:3) was 5.18, which indicates the composite is in a neutral charge. Qin et al. (2015) reported that at a pH value below pHpzc, the composite surface charge tends to be positive, degrading anionic dyes. In contrast, when the pH value is above pHpzc, the surface charge tends to be negative for degrading cationic dyes. Since the dye used in the photodegradation process was anionic, namely Remazol yellow, the photodegradation will be favorable if the pH of the solution is adjusted below pHpzc.

### Remazol Yellow Photodegradation

**Effect of Variation in Photodegradation Time.** The curve showing the effectiveness of reduction in the concentration of the Remazol yellow dye with variation in time is shown in Figure 5.

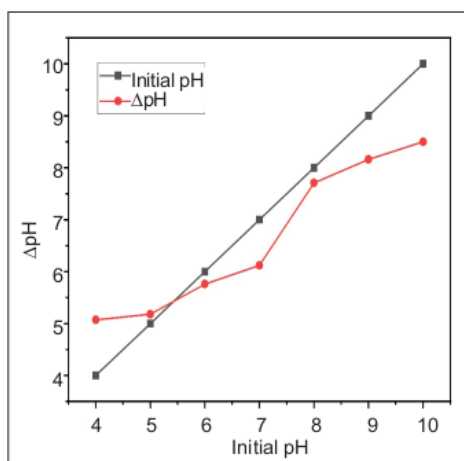


Figure 4. pHpzc SnO<sub>2</sub>-Co (2:3)

Removal of Remazol Yellow Using SnO<sub>2</sub>-Co Photocatalyst

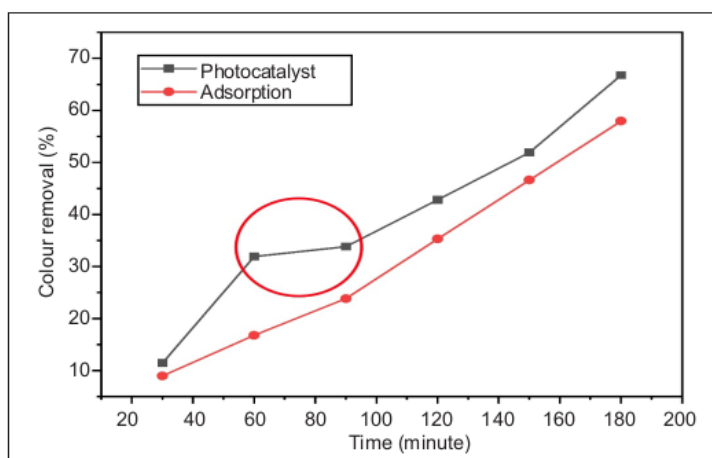


Figure 5. Effect of time on Remazol yellow removal

Based on the curve obtained in Figure 5, at 30 to 180 minutes, there was an increase in the percentage of effectiveness from 11.46 to 66.78%. This percentage shows the degraded dye; hence, the greater the value, the more degraded the Remazol yellow dye. The most effective percentage increase in reducing the dye concentration was found at 30 minutes of irradiation time. Furthermore, at 60 to 180 minutes, the percentage effectiveness of decreasing the concentration was relatively low. The ability of photocatalysts to excite electrons from the valence to the conduction band does not increase; hence, the free electrons produced are widely used to degrade intermediates in the photodegradation process (Kumar & Pandey, 2017). The irradiation time in the photodegradation process describes the length of interaction between the photocatalyst and UV light to produce free electrons ( $e^-$ ) with holes ( $h^+$ ) and form a redox reaction that ultimately degrades the dye (Alshabanat & AL-Anazy, 2018). As shown in Figure 5, the highest percentage was at 180 minutes; therefore, it was concluded that the best time for the photodegradation of Remazol dye is at 180 minutes. Moreover, controls as a comparison were also carried out through the adsorption process of Remazol yellow or without UV light irradiation. Based on the curve in Figure 5, there was also an increase in the percentage of effectiveness in decreasing the dye concentration over time. The percentage was smaller without UV light irradiation compared to UV light irradiation of 57.94%. Therefore, the percentage difference in the effectiveness of reducing the concentration with or without UV light irradiation was not significant. The dye and the composite undergo an adsorption process before interacting with UV light during the photodegradation process. Besides, the SnO<sub>2</sub> photocatalyst is also widely used as an adsorbent in dye adsorption. Abdelkader et al. (2016) reported that SnO<sub>2</sub> is applicable as a dye adsorbent because it has a wide and dense surface; hence, its ability to absorb dye is relatively large. Paramarta et al. (2016) combined the SnO<sub>2</sub> with graphene

and nanographene to increase the adsorption capacity to degrade the Methylene blue. The results show that the SnO<sub>2</sub> composite with graphene achieves a higher adsorption capacity of about 20% than the composite with NGP. Meanwhile, a SnO<sub>2</sub>/CeO<sub>2</sub> Nano-Composite Catalyst was used to adsorb the Alizarin Dye. The removal efficiencies of Alizarin-3-methylimino-diacetic acid, alizarin yellow, and alizarin red S dyes were showed 95.0%, 95.3%, and 87.8%, respectively (Hassan et al., 2020).

**Effect of Variation in Initial Concentration of Remazol Yellow.** The effectiveness of decreasing Remazol yellow concentration with variations in the initial concentration of the dye is shown in Figure 6.

Based on the curve obtained in Figure 6, the lowest reduction of Remazol yellow is at a concentration of 10 ppm, namely 74.41%. The most effective percentage, which ranged from 10 to 20 ppm, decreased from 74.41 to 64.46%, but at 25 to 30 ppm, the percentage increased from 67.57 to 71.04%. Wahyuningsih et al. (2017) stated that the higher the concentration of the dye used, the larger the number of the molecules, affecting the interaction between the catalyst and UV light. Dyes with large concentrations tend to have a darker color, thereby blocking UV rays for the catalyst. The minimum interaction between UV light and the catalyst produced less photon energy; hence, the catalyst tends to act as an adsorbent at a large dye concentration. Comparative control was also carried out on the effect of variations in the initial concentration of the dye using adsorption or without UV light irradiation. Based on the curve in Figure 6, the largest reduction in the dye concentration was at 30 ppm, with a percentage of 58.96%. This composite is potential in dye removal, and it can be compared with other methods, as Purnawan et al. (2021). Meanwhile, Shu et al. (2015) stated that the higher the concentration, the greater the amount of dye adsorbed on the composite surface.

It is consistent with the data obtained in the adsorption process of Remazol yellow using the SnO<sub>2</sub>/Co composite with or without UV light irradiation. Based on the results, the reduction effectiveness with UV light irradiation or photodegradation was greater than that of adsorption without UV light irradiation. It is because the light from the UV lamp interacts with the photocatalysts, which in turn degrades the Remazol yellow solution. Therefore, the decrease in concentration is greater compared to the use of SnO<sub>2</sub>-Co, which only absorbs particles on the surface.

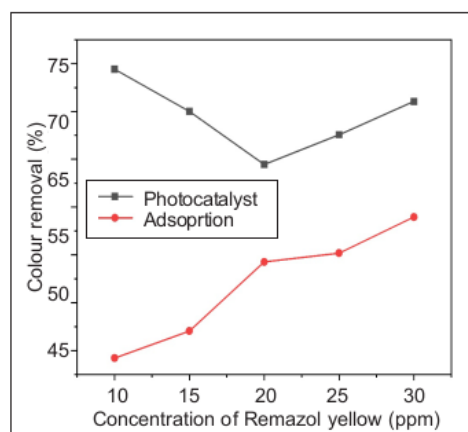


Figure 6. Effect of initial dye concentration of Remazol yellow removal

## CONCLUSION

SnO<sub>2</sub>/Co composites with mass ratios of (2:1), (2:2), and (2:3) were successfully synthesized, and the characterization results using XRD showed similarities with the typical peak of the JCPDS card No. data. 41-1445 at 2θ of 33°. The UV-Vis DRS characterization results for SnO<sub>2</sub> showed an energy bandgap of 3.05 eV, while the SnO<sub>2</sub>/Co composite (2:3) was 2.8 eV. Furthermore, the surface morphology of the SnO<sub>2</sub>/Co composite (2:3) determined using SEM characterization showed an uneven round surface and forms pores caused by an aggregate of Co doping on the surface of SnO<sub>2</sub> with the constituent percentage of 61.24, 24.67, and 14.09% for Sn, O, and Co respectively. Therefore, the optimal condition for the reduction in the concentration of Remazol yellow was at 180 minutes contact time and 10 ppm for the initial concentration with the highest percentage of 66.78 and 74.41%, respectively.

## ACKNOWLEDGMENT

The author is grateful to Universitas Sriwijaya for the financial support through Hibah Unggulan Kompetitif 2020 Contract No. 0216.050/UN9/SB3.LPPM.PT/2020.

## REFERENCES

- Abdelkader, E., Nadjia, L., & Rose-Noelle, V. (2016). Adsorption of Congo red azo dye on nanosized SnO<sub>2</sub> derived from Sol-gel method. *International Journal of Industrial Chemistry*, 7, 53-70. <https://doi.org/10.1007/s40090-015-0061-9>
- Akti, F. (2018). Photocatalytic degradation of remazol yellow using polyaniline-doped tin oxide hybrid photocatalysts with diatomite support. *Applied Surface Science*, 455, 931-939. <https://doi.org/10.1016/j.apsusc.2018.06.019>
- Akti, F., & Balci, S. (2022). Synthesis of APTES and alcohol modified Sn/SBA-15 in presence of competitive ion: Test in degradation of remazol yellow. *Materials Research Bulletin*, 145, Article 111496. <https://doi.org/10.1016/j.materresbull.2021.111496>
- Alshabanat, M. N., & AL-Anazy, M. M. (2018). An experimental study of photocatalytic degradation of Congo red using polymer nanocomposite films. *Journal of Chemistry*, 2018, Article 9651850. <https://doi.org/10.1155/2018/9651850>
- Attar, A. S. (2018). Efficient photocatalytic degradation of methylene blue dye by SnO<sub>2</sub> nanotubes synthesized at different calcination temperatures. *Solar Energy and Solar Cell*, 183, 16-24. <https://doi.org/10.1016/j.solmat.2018.03.046>
- Ba-Abbad, M. M., Takriff, M. S., Said, M., Benamor, A., Nasser, M. S., & Mohammad A.W. (2017). Photocatalytic degradation of pentachlorophenol using ZnO nanoparticles: Study of intermediates and toxicity. *International Journal of Environmental Research*, 11, 461-473. <https://doi.org/10.1007/s41742-017-0041-3>

- Bhagwat, A. D., Sawant, S. S., Ankamwar, B. G., & Mahajan, C. M. (2015). Synthesis of nanostructured tin oxide (SnO<sub>2</sub>) Powder and tin films by sol-gel method. *Journal of Nano and Electronic Physics*, 7(4), 1-4.
- Bhuiyan, M. S. H., Miah, M. Y., Paul, S. C., Aka, T. D., Saha, O., Rahaman, M. M., Sharif, M. J. I., Habiba, O., & Ashaduzzaman, M. (2020). Green synthesis of iron oxide nanoparticle using Carica papaya leaf extract: Application for photocatalytic degradation of remazol yellow RR dye and antibacterial activity. *Heliyon*, 6(8), Article e04603. <https://doi.org/10.1016/j.heliyon.2020.e04603>
- Bouaïne, A., Brihi, N., Schmeber, G., Ulhaq-Bouillet, C., Colis, S., & Dinia, A. (2007). Structural, optical and magnetic properties of co-doped SnO<sub>2</sub> powders synthesized by the coprecipitation technique. *Journal of Physical Chemistry C*, 111(7), 2924-2928. <https://doi.org/10.1021/jp066897p>
- Guezzen, B., Didi, M. A., & Medjahed, B. (2018). Sorption of Congo red from aqueous solution by surfactant-modified bentonite: Kinetic and factorial design study. *International Journal of Chemical and Molecular Engineering*, 12(3), 149-156. <https://doi.org/10.5281/zenodo.1316193>
- Handayani, D. S., Purnawan, C., Pranoto., Hastuti, S., & Hilmiyana, D. (2016). Adsorption of remazol yellow from aqueous solution on chitosan-linked P-T-Butylcalix[4]Arene. In *IOP Conference Series: Materials Science and Engineering* (Vol. 107, Issue 1, Article 012011). IOP Publishing Limited. <https://doi.org/10.1088/1757-899X/107/1/012011>
- Hassan, S. S. M., Kamel, A. H., Hassan, A. A., Amr, A. E. E., Naby H. A., & Elsayed, E. A. (2020). A SnO<sub>2</sub>/CeO<sub>2</sub> nano-composite catalyst for alizarin dye removal from aqueous solutions. *Nanomaterials*, 10(2), Article 254. <https://doi.org/10.3390/nano10020254>
- Ibarguen, C. A., Mosquera, A., Parra, R., Castro, M. S., & Rodríguez-Páez, J. E. (2007). Synthesis of SnO<sub>2</sub> nanoparticles through the controlled precipitation route. *Material Chemistry and Physics*, 101(2-3), 433-440. <https://doi.org/10.1016/j.matchemphys.2006.08.003>
- Kumar, A., & Pandey, G. (2017). A review on the factors affecting the photocatalytic degradation of hazardous materials. *Material Science & Engineering International Journal*, 1(3), 106-114. <https://doi.org/10.15406/mseij.2017.01.00018>
- Lokhand, P. E., & Panda, H. S. (2015). Synthesis and characterization of CoNi(OH)<sub>2</sub> material for supercapacitor application. *International Advanced Research Journal in Science*, 2(9), 10-14.
- Malvankar, S., Doke, S., Gahlaut, R., Martinez-Teran, E., El-Gendy, A.A., Deshpande, U., & Mahamuni, S. (2020). Co-doped SnO<sub>2</sub> nanocrystals: XPS, raman, and magnetic studies. *Journal of Electronic Materials*, 49, 1872-1880. <https://doi.org/10.1007/s11664-019-07865-5>
- Mani, R., Vivekanandan, K., & Vallalperuman, K. (2016). Synthesis of pure and cobalt (Co) doped SnO<sub>2</sub> nanoparticles and its structural optical and photocatalytic properties. *Journal of Materials Science: Material in Electronics*, 28, 4396-4402. <https://doi.org/10.1007/s10854-016-6067-z>
- Mohammed, H. A., Sanaullah, K., Soh, F. L., Andrew Ragai, H. R., Hamza, A., & Khan, A. (2017). Modeling and optimization of photocatalytic treatment of pre-treated palm oil mill effluent (POME) in a UV/TiO<sub>2</sub> system using response surface methodology (RSM). *Cogent Engineering*, 4(1), Article 1382980. <https://doi.org/10.1080/23311916.2017.1382980>
- Naje, A. N., Norry, A. S., & Suhail, A. M. (2013). Preparation and characterization of SnO<sub>2</sub> nanoparticles. *International Journal of Innovative Research in Science Engineering and Technology*, 2(12), 7068-7072.

- Paramarta, V., Taufik, A., & Saleh, R. (2016). Better adsorption capacity of SnO<sub>2</sub> nanoparticles with different graphene addition. *Journal of Physics: Conference Series*, 776(1), Article 012039. <http://dx.doi.org/10.1088/1742-6596/776/1/012039>
- Peng, T., Zhao, D., Dai, K., Shi, W., & Rao, K. (2005). Synthesis of titanium dioxide nanoparticles with mesoporous anatase wall and high photocatalytic activity. *Journal of Physical Chemistry B*, 109(11), 4947-4952. <https://doi.org/10.1021/jp044771r>
- Pirmoradi, H., Malakootikhah, J., Karimipour, M., Ahmadpour, A., Shahtahmasebi, N., & Koshky, E. F. (2011). Study of cobalt-doped SnO<sub>2</sub> thin films. *Middle-East Journal of Scientific Research*, 8(1), 253-256.
- Purnawan, C., Wahyuningsih, S., Aniza, O. N., & Sari, O. P. (2021). Photocatalytic degradation of remazol brilliant blue R and remazol yellow FG using TiO<sub>2</sub> doped Cd, Co, Mn. *Bulletin of Chemical Reaction Engineering & Catalysis*, 16(4), 804-815. <https://doi.org/10.9767/bcrec.16.4.11423.804-815>
- Qamar, M. A., Shahid, S., Khan, S. A., Zaman, S., & Sarwar, M. N. (2017). Synthesis characterization optical and antibacterial studies of co-doped SnO<sub>2</sub> nanoparticles. *Digest Journal of Nanomaterials and Biostructures*, 12(4), 1127-1135.
- Qin, X., Liu, F., Wang, G., & Huang, G. (2015). Adsorption of humic acid from aqueous solution by hematite: Effect of pH and ionic strength. *Environmental Earth Sciences*, 73, 4011-4017. <https://doi.org/10.1007/s12665-014-3686-7>
- Ragupathy, S., & Ramamoorthy, M. (2021). A study on Co doped SnO<sub>2</sub> loaded corn cob activated carbon for the photocatalytic degradation of methylene blue dye. *Research Square*, 40(1), 1-20. <https://doi.org/10.21203/rs.3.rs-168313/v1>
- Rukkumani, V., Devarajan, N., & Saravanakumar, M. (2017). Fabrication of sram memory devices using co-doped SnO<sub>2</sub> nanoparticles. *Journal of Ovonic Research*, 13(1), 1-5.
- Saravanakumar, M., Jeevitha, N., & Prabakaran, K. (2016). Structural and luminescence characteristics of nanocrystalline SnO<sub>2</sub> doped with Co<sup>2+</sup>. *Journal of Ovonic Research*, 12(4), 209-214.
- Shah, M. P., Patel, K. A., Nair, S. S., & Darji, A. M. (2013). Microbial decolorization of methyl orange dye by *Pseudomonas Sp. OA Biotechnology*, 2(1), Article 10. <https://doi.org/10.13172/2052-0069-2-1-497>
- Sharma, J., Vashishtha, M., & Shah, D. O. (2014). Crystallite size dependence on structural parameters and photocatalytic activity of microemulsion mediated synthesized ZnO nanoparticles annealed at different temperatures. *Global Journal of Science Frontier Research: B Chemistry*, 14(5), 18-32.
- Shu, J., Wang, Z., Huang, Y., Huang, N. R. C., & Zhang, W. (2015). Adsorption removal of Congo red from aqueous by polyhedral Cu<sub>2</sub>O nanoparticles: Kinetics, isotherms dan thermodynamics mechanism analysis. *Journal of Alloys and Compounds*, 633, 338-346. <https://doi.org/10.1016/j.jallcom.2015.02.048>
- Sivakarhik, P., Thangraj, V., Perumalraj, K., & Balaji, J. (2016). Synthesis of co-doped tin oxide nanoparticles for photocatalytic degradation of synthetic organic dyes. *Digest Journal of Nanomaterials and Biostructures*, 11(3), 935-943.
- Sudha, D., & Sivakumar, P. (2015). Review on the photocatalytic activity of various composite catalysts. *Chemical Engineering and Processing: Process Intensification*, 97, 112-133. <https://doi.org/10.1016/j.cep.2015.08.006>

Muhammad Said, Fahma Riyanti, Poedji Loekitowati Hariani, Sastriani and Widya Twiny Rizki

- Wahyuningsih, S., Estiningsih, P., Anjani, V., Saputri, L. N. M. Z., Purnawan, C., & Pramo, E. (2017). Enhancing remazol yellow FG decoloration by adsorption and photoelectrocatalytic degradation. *Molekul*, *12*(2), 126-132. <http://dx.doi.org/10.20884/1.jm.2017.12.2.321>
- Wan, N., Lu, X., Wang, Y., Zhang, W., Bai, Y., Hu, Y. S., & Dai, S. (2016). Improved Li storage performance in SnO<sub>2</sub> nanocrystals by a synergetic doping. *Scientific Reports*, *6*(1), Article 18978. <https://doi.org/10.1038/srep18978>
- Yehia, M., Labib, S., & Ismail, S. M. (2019). Structural, optical and magnetic properties of co-doped SnO<sub>2</sub> nanoparticles. *Journal of Electronic Materials*, *48*, 4170-4178. <https://doi.org/10.1007/s11664-019-07179-6>

PREPRINT

# Removal of Remazol Yellow

---

## ORIGINALITY REPORT

---

**23%**

SIMILARITY INDEX

**6%**

INTERNET SOURCES

**22%**

PUBLICATIONS

**5%**

STUDENT PAPERS

---

## MATCH ALL SOURCES (ONLY SELECTED SOURCE PRINTED)

---

1%

★ Yawen Wang, Lizhi Zhang, Kejian Deng, Xinyi Chen, Zhigang Zou. " Low Temperature Synthesis and Photocatalytic Activity of Rutile TiO Nanorod Superstructures ", The Journal of Physical Chemistry C, 2007

Publication

---

Exclude quotes Off

Exclude matches Off

Exclude bibliography Off